Bell, V.A.; Kay, A.L.; Jones, R.G.; Moore, R.J.; Reynard, N.S.. 2009 Use of soil data in a grid-based hydrological model to estimate spatial variation in changing flood risk across the UK. *Journal of Hydrology*, 377 (3-4). 335-350.
10.1016/j.jhydrol.2009.08.031

Use of soil data in a grid-based hydrological model to estimate spatial variation in changing flood risk across the UK

V.A. Bell[1], A.L. Kay[1], R.G.Jones[2], R.J Moore[1], N.S Reynard[1]

[1]Centre for Ecology and Hydrology, Wallingford, Oxfordshire, OX10 8BB, UK

[2]Met Office Hadley Centre (Reading Unit), Meteorology Building, University of Reading, Reading, RG6 6BB, UK

Corresponding author. Tel: +44 1491 692264

E-mail address: vib@ceh.ac.uk (V.A. Bell).

Summary

A grid-based flow routing and runoff-production model, configured to employ as input either observed or Regional Climate Model (RCM) estimates of precipitation and potential evaporation (PE), has previously been used to assess how climate change may impact river flows across the UK. The slope-based Grid-to-Grid (G2G) model adequately simulated observed river flows under current climate conditions for high relief catchments, but was less successful when applied to lower-relief and/or groundwater-dominated areas. The model has now been enhanced to employ a soil dataset to configure the probability-distributed store controlling soil-moisture and runoff generation within each grid-cell. A comparison is made of the ability of both models to simulate gauged river flows across a range of British catchments using observations of rainfall and PE as input. Superior performance from the enhanced G2G formulation incorporating the soil dataset is demonstrated.

Following the model assessment, the observed precipitation and PE data used as input to both hydrological models were replaced by RCM estimates on a 25 km grid for a Current (1961 to 1990) and a Future (2071 to 2100) time-slice. Flood frequency curves derived from the flow simulations for the two time-slices are used to estimate, for the first time, maps of changes in flood magnitude for all river points on a 1 km grid across the UK. A high degree of spatial variability is seen in the estimated change in river flows, reflecting both projected climate change and the influences of landscape and climate variability. These maps also highlight large differences between the climate impact projections arising from the two models. The improved structure and performance of the soil-based G2G model adds confidence to its projections of flow changes being realistic consequences of the climate change scenario applied. A resampling method is used to identify regions where these projections may be considered robust. However, with the climate change scenario used representing only one plausible evolution of the future climate, no clear message can be drawn here about projected river flow changes.

KEYWORDS

Rainfall-runoff model; Regional climate model; flood frequency: climate change

Introduction

An analysis of precipitation records over the period 1961 to 2000 (Osborn and Hulme, 2002) indicates that UK precipitation has tended to become more intense in winter and less intense in summer. The impact of such changes in rainfall on river flows will depend on both the nature of the rainfall and the physical characteristics of the catchment. For fast-responding catchments, such as those in impermeable or high relief areas, the features of the specific rainfall event are critical. Such catchments tend not to have the deep soils or permeable geology that lead to the long-term hydrological “memory” often exhibited by larger lowland rivers. Many drainage areas in Southeast England, including the Thames Basin, are typical of lowland catchments where the long-term balance between rainfall and evaporation can have an important influence on flood response to storm rainfall.

Over the past thirty to forty years there has been some evidence of a positive trend in high river flow indicators in the maritime–influenced upland areas of North and West Britain (Hannaford and Marsh, 2008). Such trends are generally thought to be linked to changes in winter precipitation arising from changes in atmospheric circulation patterns. However "little compelling evidence" was found for a trend towards higher flows in lowland areas of South and East Britain. Analyses of much longer flow records spanning the 20th century (Black, 1996; Robson, 2002; Hannaford and Marsh, 2008) have so far detected no apparent *long-term* trend in UK flood magnitude. Hannaford and Marsh (2008) note that over the last century the increasing temperatures observed in the UK are likely to have directly influenced key processes affecting floods: notably a decrease in snowmelt-induced floods and occurrence of frozen ground since the 1960s, and temperature-induced changes in evaporation (which can affect soil moisture deficits and flood generation).

Current UK guidance on how to consider the potential impacts of climate change on flood flows when planning flood defence schemes states that *"The limited number of catchments researched to date supports applicability of a 20% allowance to the 2080s for peak river flow"* (Defra, 2006). Most research investigations into the effects of climate change on UK river flows, including that which led to the Defra (2006) guidance for flood defences, have used catchment hydrological models to provide estimates of changes in flow for a single location, or a small set of locations: examples are Kay *et al.* (2009), New *et al.* (2007), Fowler and Kilsby (2007), Wilby and Harris (2006), Wilby *et al.* (2006), Nawaz and Adeloye (2006), Cameron (2006), Kay *et al*. (2006), Arnell (2003) and Reynard *et al*. (2004). Generally, the hydrological model is calibrated to catchment conditions, using model parameters to adjust the modelled catchment response to rainfall, in order to allow for the spatial heterogeneity of soil, geology, topography and land-cover. The model parameters can also be adjusted to take into account artificial influences on flows, such as water abstraction.

Here we use a single, grid-based model (Grid-to-Grid, or G2G) and a single set of parameters for the whole of the UK to simulate the different responses of catchments to rainfall and evaporation, using digital datasets of landscape properties to provide the spatial differentiation. In order to determine the effect of hydrological model structural quality on river flows, estimates from an enhanced G2G model, which includes the effect of soil properties on runoff production, are compared to those from the slope-dependent G2G model used in previous assessments of changing flood risk (Bell *et al.*, 2007a,b). These two model variants are distinguished here using the names 'Soil-G2G' and 'Slope-G2G' respectively. Estimates of river flows from both model variants are compared to observed flows for a large set of catchments using historical observations of rainfall and potential evaporation (PE) as model input. Model performance for different sizes and types of catchment across Britain is assessed. Bell *et al.* (2007a) found that the Slope-G2G provided reasonably good flow estimates for high relief catchments, but was less effective in areas of lower relief or where groundwater processes have a significant influence on river flows. The enhanced G2G model formulation presented here attempts to overcome these deficiencies, and contains further developments to the prototype Soil-G2G formulation previously trialled in some Upper Thames catchments (Moore *et al.*, 2007, 2006a,b).

Use of a grid-based hydrological model in conjunction with high-resolution climate model output has made it possible here, for the first time, to estimate the spatial effects of climate change on peak river flows across the UK. Observations of rainfall and PE used to calibrate and assess both hydrological models are replaced by Regional Climate Model (RCM) estimates on a 25 km grid and at hourly intervals (daily for PE) for a Current (1961 to 1990) and a Future (2071 to 2100) time-slice. Flood frequency curves derived from the flow simulations for both time-slices are used to produce maps of changes in flood magnitude for river points on a continuous 1 km grid across the UK. These maps indicate a high degree of spatial variability in the sensitivity of UK rivers to future changes in climate. The resilience, or "robustness", of the modelled changes in flood magnitude is investigated using a resampling method. Areas of the UK are identified for which confidence in the projected changes under this regional climate model scenario is greatest.

The hydrological models

Two hydrological model formulations are compared, one for which runoff production is parameterised in terms of slope (Slope-G2G), and one which introduces the effects of soil/geology on runoff production and catchment response (Soil-G2G). The models can be configured for use at (almost) any spatial resolution, with the temporal resolution determined by numerical stability criteria. They are run here at a 1 km resolution and for a 15 minute time-step over a UK model domain. The models employ Digital Terrain Model (DTM) data to support their configuration and parameterisation. A modular formulation allows model revisions and extensions to be made. In order to represent spatial heterogeneity within each 1 km grid-cell, and to ensure that each cell generates realistic quantities of saturation-excess runoff even when it is not fully saturated, the probability-distributed soil moisture store formulation of Moore (1985, 2007) has been invoked in both models. Runoff from a cell soil column is considered to consist of the saturation-excess surface flow and the groundwater sub-surface flow. These runoffs from each cell form the lateral inflows to the G2G flow routing scheme. The scheme as presented in Bell *et al.* (2007a) consists of a kinematic wave formulation for routing both surface and sub-surface gridded runoffs. This scheme has been further enhanced to include dependence on river width and slope when used to represent river channel flow processes.

The G2G can be used in two ways: first as an area-wide model providing flow estimates over a large region, and secondly as a catchment model which may be calibrated to obtain the best possible agreement between modelled and observed flows. As an area-wide model, the G2G can be less accurate for a particular catchment than a model specifically calibrated to the catchment, but is well suited to support river flow simulation at any set of locations within a region. As a consequence, the models are able to be calibrated to groups of gauged locations within a region and river flow simulations extracted for any ungauged location within the same area.

The structure and performance of the two formulations of the G2G model, with area-wide calibrations, is assessed here with reference to observed flow records for catchments across Britain. Model performance will impact on the quality of the flood frequency curves derived from the river flow simulations and on the reliability of the assessment of change in flood frequency under a future climate.

A description of each G2G model formulation follows. The Slope-G2G has already been presented in detail (Bell *et al.,* 2007a), so only a brief description is provided here for comparison with the Soil-G2G.

The Soil-G2G: a distributed grid-based model incorporating soil information

Consider a sloping soil column of depth L and slope s_0 subject to precipitation falling at a rate p and with an evaporation rate E_a as shown in Figure 1. Some of the rainwater entering the soil column can drain laterally to adjacent grid-squares, while saturation-excess flow contributes to surface runoff. Water also moves downwards via percolation and drainage which eventually contributes to groundwater (sub-surface) flow.

Soil-moisture and surface runoff-production in the Soil-G2G

The actual, maximum 'available' and residual water storages (water depth per unit area) in the soil column are given by

$$S = (\theta - \theta_r)L \qquad (1)$$

$$S_{\max} = (\theta_s - \theta_r)L\,, \qquad (2)$$

$$S_r' = \theta_r L \qquad (3)$$

where θ, θ_s and θ_r are the actual, saturation and residual water contents (water volume per unit volume of soil). The total water stored is denoted $S' = S + S'_r$, which can take a maximum value of $S'_{\max} = S_{\max} + S'_r$. The residual water S'_r held under tension forces is not available for drainage but can contribute to evaporation.

Let $V = \Delta x^2 S$ denote the volume of available water stored in the unsaturated layer of the soil column of a given grid-square cell of side length Δx. From continuity, the rate of change in water volume is given by

$$\frac{dV}{dt} = (p - E_a)\Delta x^2 + q_i - q_L - q_p - q_s, \qquad (4)$$

where q_i is the rate of inflow to the cell from contributing upstream cells, q_L is the lateral drainage rate from the cell, q_p is the downward percolation (drainage) rate to the saturated zone and q_s is saturation-excess surface runoff. This equation of continuity is also used in the Slope-G2G formulation, but with $q_L = 0$.

The lateral drainage rate, q_L, is given by

$$q_L = \frac{C\Delta x}{\Delta x^{2\alpha}} V^\alpha = C\Delta x S^\alpha. \qquad (5)$$

The conveyance term C is given by $C = Lk_s^L s_0 / S_{\max}^\alpha$, where s_0 is the local slope (derived from digital elevation data) and k_s^L is the lateral saturated hydraulic conductivity. A similar equation can be derived by integrating the Brooks-Corey (1964) relation for hydraulic conductivity over the depth of soil column (Todini, 1995; Benning, 1995) with parameter α the pore-size distribution factor (here, taken to be unity).

Percolation (a vertical downward flow from the soil column), q_p, is represented as a simple power law function of the available soil water volume V, expressed as a fraction of the saturated water volume $V_{\max}$,

$$q_p = k_s^v \Delta x^2 \left(\frac{V}{V_{\max}} \right)^{\alpha_p} = k_s^v \Delta x^2 \left(\frac{S}{S_{\max}} \right)^{\alpha_p}, \tag{6}$$

where k_s^v is the vertical saturated hydraulic conductivity of the soil and α_p is the exponent of the percolation function. Clapp and Hornberger (1978) indicate, on the basis of soil experiments, that α_p can vary from circa 11 for sand to 25 for clay. Following tests, a constant value for α_p of 15 is assumed here (in the absence of a suitable spatial dataset).

The dependence of evaporation loss on total soil moisture content is introduced by assuming the following simple function between the ratio of actual to potential evaporation, E_a / E, and soil moisture deficit, $S_{\max} - S$:

$$\frac{E_a}{E} = 1 - \left\{ \frac{(S_{\max} - S)}{S_{\max} + S_r'} \right\}^{b_e}. \tag{7}$$

Note that evaporation can occur from water held under soil tension. This formulation was used within the PDM (Moore, 1985, 2007) where a value of b_e=2.5 is often recommended to obtain realistic variation in evaporation between seasons; this value has been used here.

In order to ensure that a grid-square generates realistic quantities of saturation-excess surface runoff q_s even when it is not fully saturated, the probability-distributed soil moisture store formulation of Moore (1985, 2007) has been invoked within each grid-square. This probability-distributed approach also forms the basis of the Xinanjiang model (Zhao et al., 1980), the Arno model (Todini, 1996) and the VIC land-surface model (Wood *et al*., 1992); an historical perspective citing earlier works is given by Moore (1985). The conceptualisation represents the spatial variation in water absorption capacity with soil, geology, land-cover and topography across the grid-square by assuming the grid-square contains a *distribution of store depths*, c, with the depths dependent upon saturation and residual soil moisture. The distribution is assumed to be of Pareto form with distribution function $F(c) = 1-(1-c/c_{\max})^b$ defined by two parameters: $c_{\max}$ the maximum store depth and b the spatial distribution (shape) parameter controlling the nature of the variation of store depth between 0 and $c_{\max}$.

Total soil moisture, $S'(t) \equiv S + S'_r$, and surface runoff, $q_s \equiv q(t)$, are evaluated at each time-step. The maximum total storage $S'_{\max} \equiv S_{\max} + S'_r$ is estimated from soil data on local saturation and the depth of the soil column. The variable $C^* \equiv C^*(t)$ is the critical capacity below which all stores are full at some time t. The proportion of the grid-square containing stores of capacity less than or equal to C^* is $\mathrm{prob}(c \le C^*) = F(C^*) = \int_o^{C^*} f(c)dc = 1-(1-C^*/c_{\max})^b$. This is the proportion of the grid-square from which the surface runoff q_s is generated when net rainfall is positive.

The PDM rainfall-runoff catchment model assumes a single distribution of stores across a catchment, with the values of b and $c_{\max}$ determined through calibration with reference to observed river flows. In contrast, the Slope-G2G exploits a relation between store capacity and terrain slope to estimate the values of b and $c_{\max}$ from DTM-derived slope data for each model grid-square (see section on Slope-G2G). For the Soil-G2G, a method to estimate b directly from soil properties, rather than through terrain slope, was sought. Parameter values obtained by calibration of the standard PDM lumped catchment model across a range of catchments, indicate that those with larger store capacity (large $S'_{\max}$) do tend to have smaller values of b, whereas those with shallow soils tend to have larger values of b. Results are shown in Fig. 2 for 37 catchments across the UK and simple curve fitting indicates that the inverse square-root relationship

$$b = 5.2/\sqrt{S'_{\max}}\,, \tag{8}$$

provides a reasonable approximation (coefficient of determination of 0.66). Soil data were used to provide an estimate of the total water stored $S'_{\max}$ from which b is then calculated using Eq. (8); this is done for each grid-square over the model domain. Trials indicated that the relationship of Eq. (8) performed well except in areas with permeable geology such as chalk downland. For these areas where stores are particularly deep ($L > 1$ m), setting $b = 0$ had the effect of removing rapid fluctuations in surface runoff and resulted in more realistically modelled river flows. For this case, all stores in a grid-square have the same capacity, c_{max}.

Estimates for the four soil properties θ_s, θ_r, L and k_s (the saturated hydraulic conductivity) are available from soil datasets for the UK at a 1 km resolution (details are provided in a later section). The vertical component of the saturated hydraulic conductivity k_s^v is assumed to be linearly related to k_s, through the relation $k_s^v = \lambda k_s$, where λ is treated as a spatially invariant model parameter referred to as the drainage conductivity multiplier. This additional parameter is required to take into account the vertical variation in hydraulic conductivity not encompassed by values taken from the UK datasets. The lateral saturated hydraulic conductivity, k_s^L, is unknown but following initial trials of the G2G, it is assumed to be related to k_s via the relation $k_s^L = 50 k_s$: this produces a moderate improvement in the timing of flow peaks in groundwater-dominated catchments. However, more extensive calibration has proved impossible, in part because most of the groundwater-dominated catchments in this study are subject to abstraction and/or uncertainty about the extent of the sub-surface catchment.

The facility exists to include a reduction of soil depth L from those provided by national datasets, for grid-cells containing significant urban and suburban areas, through use of the LCM2000 spatial dataset of land-cover (Fuller *et al.,* 2002). The soil depth is multiplied by the factor $1 - 0.7\phi_u - 0.3\phi_s$ where ϕ_u and ϕ_s are the fractions of urban and suburban area within each grid cell. This reduction in soil storage will have the effect of increasing runoff, particularly surface runoff, in urban areas leading to a faster response to rainfall. This responsiveness has been further enhanced through the use of an increased routing speed in urban areas (see Section *Estimation of river flows by surface and channel flow routing models*).

Sub-surface runoff-production in the Soil-G2G

It is assumed that percolation freely drains as recharge to the groundwater saturated zone (for the cell), so that the recharge rate $q_r \equiv q_p$. Let V_g denote the groundwater volume stored in the cell and s_b the slope of the underlying bedrock in the flow direction. Continuity for the groundwater volume is

$$\frac{dV_g}{dt} = q_p - q_g \tag{9}$$

where q_g is the lateral groundwater flow from the cell. Darcy's law gives the lateral groundwater flow out of the cell to a reasonable approximation by the linear relation

$$q_g = \frac{k_g s_b}{\Delta x} V_g \tag{10}$$

where k_g is the horizontal hydraulic conductivity of the aquifer. This is appropriate for a confined aquifer. However, suitable values for bedrock slope, s_b, and conductivity, k_g, are not straightforward to obtain. One approach is to assume that bedrock slope mirrors the surface topographic slope which can be estimated from digital terrain data. Conductivity information may be obtained from geology datasets but obtaining meaningful values for the present scale of application may present difficulties. Geological datasets have not been used for the present model application. Instead, a nonlinear storage function relating groundwater flow to volume has been invoked, such that

$$q_g = \kappa_g V_g{}^m, \ \kappa_g > 0, \ m > 0, \tag{11}$$

where κ_g is a rate constant and m is the nonlinear power. For this application, a cubic storage function has been assumed (m =3), and κ_g is treated as a spatially invariant parameter for estimation.

Estimation of river flows by surface, subsurface and channel flow routing models

Runoff from the soil column is considered to consist of the saturation-excess flow, q_s, and groundwater flow, q_g. These runoffs from each cell form the lateral inflows to the Grid-to-Grid flow routing scheme comprising of two parallel coupled equations representing the surface and subsurface flow pathways respectively. The scheme (Bell *et al.,* 2007a,b) employs a kinematic wave equations in 1-dimension of the form:

$$\frac{\partial q}{\partial t} + c\frac{\partial q}{\partial x} = c(u + R) \tag{12}$$

where q is either surface or subsurface flow, R denotes return flow per unit path length (water transfer between subsurface and surface pathways), and u represents lateral inflows per unit path length, which include runoff generated by the runoff-production scheme. The wave speed c can vary with the pathway (surface or subsurface) and surface-type (land or river) combination.

Invoking forward difference approximations to the derivatives in (12) gives the discrete formulation

$$q_k^n = (1-\vartheta)q_{k-1}^n + \vartheta\left(q_{k-1}^{n-1} + u_k^n + R_k^n\right) \tag{13}$$

where k and n denote positions in discrete time and space respectively, the dimensionless wave speed $\vartheta = c\,\Delta t/\Delta x$ and $0 < \vartheta < 1$. This is a simple, explicit numerical formulation for the kinematic wave equation with u_k^n and R_k^n now the lateral inflow and return flow over the path length. This numerical scheme has the advantage of introducing diffusion (albeit numerically) and so more closely represents the propagation of actual flow through the landscape. Figure 3 summarises the key features of the coupled runoff-production and routing scheme.

This finite-difference scheme forms the basis of the routing component of both the Soil- and Slope-G2G. In each case, the routing is implemented in terms of an equivalent depth of water in the surface or sub-surface store over the grid square, S_k^n, with $q_k^n = \kappa S_k^n$ and where $\kappa = c/\Delta x$ is a rate constant with units of inverse time and Δx is the grid-cell size. The inflow and return flow are also re-expressed in terms of water depth for calculation purposes. In the Soil-G2G, return flow from the sub-surface to the surface is estimated as $R_k^n = (r_b S_{bk}^n + r_i S_{ik}^n)/\Delta t$, which includes a contribution directly from the soil column, while for the Slope-G2G return flow is a proportion of the sub-surface flow only, i.e. $R_k^n = r_b S_{bk}^n / \Delta t$. In both cases, S_{bk}^n is the depth of water in the sub-surface routing store, r_b is the return flow fraction and for the Soil-G2G, r_i is the return flow fraction from the soil store and S_{ik}^n is the depth of water in the soil column. For diagonal flow-paths the distance travelled across the grid-cell is increased by a factor of $\sqrt{2}$.

In the Soil-G2G, routing along surface pathways of river channel type employs the Horton–Izzard nonlinear storage approach (Dooge, 1973; Moore and Bell, 2001) applied to a varying width channel network (Ciarapica and Todini, 2002; Moore *et al.*, 2007) and exploits geomorphological relations developed by Bell and Moore (2004). In this case the momentum equation is given by the Manning equation $q = CS^m$, where S is the water depth, the conveyance $C = \sqrt{s_0}/n$ where s_0 is the channel bed slope and n is Manning's roughness coefficient, and $m = 5/3$. Without change of notation, to simplify presentation, this routing scheme is developed below for a river grid cell within the modelled domain.

Assuming a network structure of channel reaches with wide rectangular cross-sections of width, w, increasing downstream, then the kinematic wave routing scheme for a reach is

$$\frac{dV}{dt} = q - \frac{Cw}{(\Delta xw)^m} V^m = q - q_c . \qquad (14)$$

Here, V is the volume stored in the reach, q_c is the outflow, and the inflow q is made up of two components: the surface runoff q_s, which includes return-flows from the soil and groundwater store, and the channel inflow from upstream q_c^u. The channel bed slope, s_0, is here assumed equal to the mean slope of the grid-cell. Standard tables of Manning's n can be used to assign values to each cell if information on the type of channel is available. Alternatively, a channel ordering system, such as that due to Strahler, could be invoked with the support of a digital terrain model and used to allow roughness to decrease with increasing stream order. Here, a constant roughness has been assumed within and across all cells for simplicity. In practice, the kinematic wave routing scheme with varying cross-sectional width used here is

$$\frac{dV}{dt} = q - \frac{c_r^* \sqrt{s_0}}{\sqrt{w}} V^2 , \qquad (15)$$

where c_r^* is a routing parameter with units of $s^{-1}m^{-5/2}$.

To estimate channel width w, the approach of Bell and Moore (2004) has been followed. They obtained the following relationship for bankfull width using observations of bankfull river dimensions published by Nixon (1959) for 27 catchments across the UK ranging in size from 157 to 9948 km^2:

$$w_b = 0.9134 A^{0.5121} \left(\frac{R_{SAAR}}{1000} \right)^{1.139} , \qquad (16)$$

where A is the area drained (km^2) and R_{SAAR} is the Standard Average Annual Rainfall (mm) over this area. This has been applied to each cell containing a river channel to obtain estimates of w.

The kinematic wave routing scheme for channel flow given by equation (14) takes the general nonlinear reservoir (Horton-Izzard) form

$$\frac{dV}{dt} = u - kV^{m} \tag{17}$$

where V is the volume of water in the channel and the quantities u and k are constants within a time-step. An integral solution of this equation is available for calculation purposes based on an approximation suggested by Smith (1977) for the general case, or analytical expressions for specific cases: see Moore and Bell (2002) and Moore *et al.* (2007) for further details. For the present application, involving specifically Eq. (15), the analytical solution for the quadratic case (m=2) is used.

For the Soil-G2G the responsiveness of the catchment to rainfall in urban areas has been further enhanced by increasing the routing parameter, k, by a factor of 2 for grid-cells where the fraction of urban area, $\phi_u > 0.25$.

The slope-dependent Grid-to-Grid Model

A full description of the slope-dependent G2G model structure and its configuration to the UK is presented in Bell *et al.* (2007a). A simple runoff production scheme based on terrain slope is used following methodology developed for the CEH Grid Model (Bell and Moore, 1998a,b) to derive surface and sub-surface runoffs from gridded rainfall and potential evaporation inputs. The Slope-G2G formulation assumes that grid-cells with less steep slopes have deeper soil stores, and are less immediately responsive to rainfall than steeper areas.

At a point it is assumed that the moisture storage capacity, c, is related to the local topographic slope, s_0, such that

$$c = \left(1 - \frac{s_0}{s_0^{\max}}\right) c_{\max} , \quad (18)$$

where $s_0^{\max}$ and $c_{\max}$ are regional maximum values of slope and capacity respectively. Further, it is assumed within a grid-square that the variation in slope has a distribution function of power form such that $F(s_0) = (s_0 / s_0^{\max})^b$, $0 \le s_0 \le s_0^{\max}$. It follows from derived-distribution theory that capacity c has the Pareto distribution $F(c) = 1 - (1 - c / c_{\max})^b$ with spatial distribution (shape) parameter, b, related to the mean slope, $\bar{s}_0$, through the expression.

$$b = \frac{\bar{s}_0}{s_0 - \bar{s}_0} . \quad (19)$$

Standard PDM theory (Moore, 1985, 2007) can then be used to obtain the fraction of a grid-square that is saturated and generating runoff. Analytical expressions are available for calculating for every model time-step the volume of surface runoff and total water storage, $S'(t)$, for each grid-square. The latter has a maximum value $S'_{\max} = c_{\max} /(b+1)$. DTM data (here, available on a 50 m grid) are used to estimate $\bar{s}_0$ for each grid-square and $s_0^{\max}$, with $c_{\max}$ treated as a regional parameter to be optimised. Values for b and $S'_{\max}$ can be calculated from these for all grid-squares. No data on soil properties are required with the Slope-G2G model variant as terrain slope is used as a surrogate for the water holding capacity of the soil. The water balance calculations for the Slope-G2G take account of losses via evaporation and drainage in a similar way to that outlined for the Soil-G2G, but using a storage-dependent drainage function incorporating a soil tension threshold.

The routing component employed by the Slope-G2G has previously been outlined in the context of the Soil-G2G model variant. It essentially employs a kinematic wave formulation that is equivalent in conceptualisation to a network cascade of linear reservoirs. Surface and subsurface runoffs are routed via parallel fast and slow response pathways linked by a return flow component representing stream-soil-aquifer interactions. The terrain-following flow paths are configured using a DTM.

Model Configuration from digital datasets

The routing component of both the Slope- and Soil-G2G models requires two DTM-derived datasets:

(i) flow directions (each grid-cell can drain in only one of 8 directions),

(ii) area draining to each 1 km grid-cell

Here, the G2G model formulation is configured spatially using river networks and terrain information derived from a 50m hydrologically corrected UK DTM, the IHDTM (Morris and Flavin, 1990). The IHDTM is derived using Ordnance Survey (OS) 1:50000 digitised contours and spot heights, and digitised river networks; it has a 0.1m vertical resolution. Although the IHDTM provides an accurate 50m grid of flow-directions, the G2G routing scheme operates on a coarser 1km grid and is unable to use these fine-scale flow-directions directly. This is a common issue in broad-scale distributed modelling, and has motivated the development of a range of methods to extract low-resolution flow direction networks from high-resolution base datasets. In a recent assessment, Davies and Bell (2009) found that two derivation methods - the Network Tracing Method (NTM, Fekete *et al*., 2001), and the COTAT+ method (Paz *et al*., 2006) - produced river networks that most closely resembled the base fine-scale (50m) river networks. The COTAT+ raster-based scheme was considered slightly better at estimating catchment areas. The accuracy of the COTAT+ river network derivation method over the UK does not seem to depend greatly on the nature of the topography it is applied to. Indeed, Davies and Bell (2009) found that it performed reasonably accurately across the whole of mainland Britain. Generally the percentage error in catchment area arising from the delineation of a catchment boundary using 1km-resolution flow-directions is less than 5%, although a few catchments have larger errors.

The runoff-production schemes for both G2G formulations require gridded estimates of average terrain slope in each grid-cell. The slope of each 1 km grid-cell is determined from the mean of the 50m grid-cell slopes contained in the 1 km grid-cell, These are estimated from the elevations of the 3×3 cell neighbourhood surrounding each cell using an average maximum technique (Burrough, 1986) as implemented in ESRI ArcGIS software. Note that this measure of cell mean slope will not necessarily represent the slope of the river.

Additional data on soil properties is required by the Soil-G2G runoff-production scheme. Here, a derived quantity called the HOST (Hydrology of Soil Types) class has been used to infer estimates of soil hydraulic properties across the UK. The HOST dataset has a 1 km resolution and consists of 29 classes, encompassing soil type, hydrological response and substrate hydrogeology (Boorman *et al.,* 1995). Although this classification only provides an integer identifier for 29 different soil types, a database of derived soil attributes supports the derivation of these classes and consists of properties such as air capacity, parent material, depth to gleying and depth to slowly permeable layer. Highly derived soil properties have been extracted from a soil properties database called SEISMIC (Hallett *et al.,* 1995), available from the National Soil Resources Institute. In SEISMIC, soil series are analysed down to a depth of 1.5 m. By comparing information from SEISMIC with the HOST dataset, Ragab together with colleagues at CEH (pers. comm.) associated values of soil properties with each of the 29 HOST classes. Relevant properties are as follows:

hydraulic conductivity at saturation : k_s (cm d^{-1}),

soil depth to “C” and “R” horizons (cm), water content at field capacity, θ_{fc}: fractional volume at 5KPa,

residual water content, θ_r: half the fractional volume at 1500KPa

The soil depths to “C” and “R” horizons consist of two values. The SEISMIC User Manual defines the C-layer as “mineral substrate, relatively unweathered ‘soft’ unconsolidated material, gravel or rock rubble”, and the R-layer as “relatively unweathered, coherent rock”. The depth to the R-layer has been used here as a surrogate for soil depth. Where a value for depth to the R-layer is not available, the depth to the C-layer is used instead. In many cases (but not all), depth to the R-layer for each soil type is greater than the depth to the C-layer.

The residual soil water content, θ_r, and the saturated hydraulic conductivity, k_s, are used directly in the Soil-G2G runoff production scheme. The water content at field capacity, θ_{fc}, represents the water content below which drainage becomes negligible. As a rule of thumb (Or and Wraith, 2002), $\theta_s = 2\theta_{fc}$, where θ_s is the water content at saturation, an estimate of which is required for the Soil-G2G runoff-production scheme. However, values for θ_{fc} associated with HOST classes from SEISMIC data range from 0.25 to 0.49 and seem rather large compared to literature values which range from 0.1 for fine sand to 0.39 for clay (Dunne and Leopold, 1978). For the present purposes it is assumed that $\theta_s = 1.25\ \theta_{fc}$, which results in values of θ_s ranging from 0.31 to 0.61.

Hydrological and climate data

Observation-based data for model calibration and assessment

Both variants of the G2G model are assessed here with respect to observed flows at river gauging station sites across the UK and using gridded time-series of precipitation and potential evaporation as model input. The precipitation data were daily values on a 5km grid derived from raingauge totals by the Met Office for the period 1958 to 2002. In the present application, the G2G model runs at a 15-minute time-step, so the daily rainfall estimates are equally spread throughout the day. Potential evaporation data were monthly values on a 40 km grid obtained from the "Met Office Rainfall and Evaporation Calculation System", MORECS (Thompson *et al.* 1981, Hough and Jones, 1997). Monthly total PE estimates are spread equally throughout the month. This method is sufficient for PE input to rainfall–runoff models, since its effect on runoff production is as a cumulative control on soil water storage.

The Slope-G2G model had previously been assessed using observed (raingauge) and modelled (from an RCM driven by quasi-observed boundary conditions) rainfall data as input (Bell *et al*., 2007a). The DTM-derived river-flow routing datasets used here differ slightly to those described by Bell *et al.* (2007a,b), as derivation-methods for flow paths and catchment boundaries have since been improved. This has required minor adjustments to be made to the Slope-G2G model parameters.

Daily flow records from 42 river gauging stations across Britain have been used in the G2G model assessment. A map showing catchment boundaries and outlet locations is presented in Fig. 4. The station names and identifiers (IDs) are listed in Table 1 together with catchment area and baseflow index (bfi). The baseflow index (Institute of Hydrology, 1980) is a dimensionless measure (range 0 to 1) expressing the fraction of river flow that derives from stored sources, such as groundwater. The catchments were chosen to represent a wide range of river regime, ranging from fast-responding upland catchments (e.g. Taw, Dee) to baseflow-dominated river basins (e.g. Mimram, Lambourn). It is important to remember that artificial controls on flow, such as reservoirs and abstractions for water supply, are not yet accounted for in the G2G model. Neglecting the effect of groundwater abstractions on river flows will result in apparent overestimation of flows in affected areas, particularly during summer months. Daily mean flow data for the catchments in Table 1, originating from the Environment Agency, were obtained from the National River Flow Archive at CEH Wallingford.

The observed data record was divided into two separate periods for model calibration and assessment. The calibration period was from 28 November 1980 to 18 December 1982 following a six-month period used for model initialisation; the period used for model assessment ran from 1 January 1985 to 31 December 1993, again preceded by a six-month initialisation period.

Regional Climate Model data for climate change assessment

The RCM used is HadRM3H, here configured at a 25km resolution; a 50km version was previously employed to produce the UKCIP02 scenarios (Hulme *et al.,* 2002).

RCM-derived hourly precipitation and daily estimates of potential evaporation have been used as input to the G2G. The data are available for two time-slices:

- Current scenario from 1960 to 1990;
- Future scenario (SRES-A2; IPCC, 2000) from 2070 to 2100.

The first 9 months of each was used to initialise the hydrological model, so each time-slice contains 30 whole water years (1 October to 30 September). It should be noted that an RCM 'year' consists of just 360 days (12 months each with exactly 30 days).

HadRM3H is described in Buonomo *et al.* (2007), which compares the RCM simulations of precipitation with observations from a raingauge network over Great Britain. The comparison indicates that HadRM3H realistically simulates extreme precipitation over time-scales of one to thirty days and return periods of two to twenty years. In particular, errors are generally no larger and sometimes smaller than those in seasonal mean precipitation. Similarly, a study of extreme rainfall comparing HadRM3H output and daily raingauge records from 204 sites across the UK by Fowler *et al.* (2005) found that the RCM provided a good representation of extreme rainfall for return periods up to 50 years. The experimental run used here is a rerun at a higher resolution (25km) of one of the experiments used for UKCIP02. As RCM rainfall is representative of average rainfall over a grid-box then rainfall events at smaller spatial scales, for example localised heavy convective precipitation, will not be captured in the models. This also means that changes in events of this nature will not be represented in the future climate scenario. However, as RCM summer rainfall compares well with observations when they have been aggregated onto the model grid, then clearly the RCM is able to capture the area-averaged effect of convective rainfall.

The 25 km RCM precipitation has been downscaled to the 1 km UK National Grid using the procedure followed by Bell *et al.* (2007b). Higher spatial rainfall resolution is provided by the standard average annual rainfall (SAAR) 1 km dataset for the period 1961–1990. For each time-step, the rainfall for each RCM grid-square is multiplied by the ratio of RCM grid-square SAAR to the 1 km grid-square SAAR to provide rainfall on a 1 km grid. This determines whether some areas generally receive more or less rainfall than others, for instance as a consequence of topography. Potential evaporation (PE) has been estimated from RCM outputs in a way that is as consistent as possible with the Penman–Monteith equation (Monteith, 1965) as implemented in MORECS (Hough and Jones, 1997), but using RCM outputs instead of synoptic station measurements. The hourly rainfall (daily PE) estimates are equally spread throughout the hour (day), in line with the approach used for the model runs driven by observations.

G2G model calibration and assessment

The G2G model has been designed for area-wide application, providing estimates of river flows throughout a region, irrespective of catchment boundaries. Where possible, the model is configured to a region, in this case the UK, using gridded datasets to represent spatial heterogeneity of hydrological response across grid-cells. With the use of greater process representation and ever-more detailed datasets one might expect that less calibration would be required to achieve an accurate representation of surface and sub-surface hydrology. However, many aspects of surface-groundwater interactions are complex, scale-dependent and still not fully understood or measurable. Thus model calibration is still required to achieve better agreement between modelled and observed river flows, particularly for groundwater-dominated regions.

As the G2G model is designed for area-wide use, care has been taken not to over-calibrate the model to individual catchments for which flow observations are available. Instead, flow measurements for catchments with a predominant soil-type have been used to determine whether the hydraulic properties associated with the soil-type provide realistic estimates of the relative volumes of surface and sub-surface runoff. Manual adjustment of soil hydraulic properties (usually effective soil depths) is applied recursively to different catchments and sub-catchments until a good estimate of downstream surface- and subsurface-flow volumes across a range of soil-types is achieved. The baseflow storage rate-constant parameter, κ_g, and drainage conductivity multiplier, λ, are adjusted as part of this runoff-calibration process, although their effects are sometimes indistinguishable from the routing time-constant parameters. Generally, adjustment of soil properties has been required for soils overlying permeable geology, such as chalk, where the baseflow component of river flow is dependent on the volume of water stored in both the soil and the bedrock. With the current absence of data to support estimates of groundwater hydraulic properties, storage in these areas has been augmented by increasing the effective soil depth and assuming that the soil hydraulic properties apply at all depths. This effectively introduces a deeper unsaturated zone below the soil layer in some areas associated with chalk and Oolite formations. In time, greater availability of soil and geological data should provide additional information to underpin model constructs of this kind.

Parameters governing the temporal development of flow peaks are determined by manual calibration to observed flows at a number of locations. These consist of time-constants for both the surface and sub-surface routing pathways, together with the return-flow fractions, r_i and r_b, which determine the proportion of sub-surface water that passes into the river at each time-step.

The same calibration/assessment procedure was followed for both the Slope-G2G and the Soil-G2G model variants. The results obtained for the nine-year assessment period are shown in Fig. 5. Here, differences between observed and modelled daily mean flows for each catchment in Table 1 are expressed in terms of the R^2 statistic, also referred to as the "Nash-Sutcliffe Efficiency" (Nash and Sutcliffe, 1970) or simply "Model Efficiency". This is defined as

$$R^2 = 1 - \frac{\sum (Q_t - q_t)^2}{\sum (Q_t - \overline{Q})^2}, \qquad (20)$$

where Q_t is the observed flow at time t, q_t is the simulated flow and $\overline{Q}$ is the mean of the observed flows over the n values involved in the summations. The R^2 statistic provides a dimensionless performance measure which expresses the proportion of variability in observed flows accounted for by the model simulation. A value of 1 indicates a perfect fit whilst a value of 0 indicates that the model is only as good as using the mean flow for model simulation. Note that R^2 can be negative if the model simulations are worse than that provided by the mean flow (assumed unknown when doing the model simulation). In the bar-charts of Fig. 5, negative R^2 values are indicated with a token value of -0.05 for clarity. In all but three of the catchments, use of the Soil-G2G leads to a more accurate simulation of observed river flows, even in high relief areas where the Slope-G2G can be particularly effective. In the figure, the catchments are displayed in ascending order of their *bfi*: this serves to highlight the better performance of the Soil-G2G in catchments where a larger proportion of the river flow derives from stored sources such as groundwater (i.e. where *bfi* is higher).

Figure 6 presents hydrographs highlighting the improved performance of the Soil-G2G in two very different catchments; the Beult at Stile Bridge (*bfi* = 0.24) and the Lambourn at Shaw (*bfi* = 0.97). The enhanced simulation performance in the Lambourn is evident: however there is still room for improvement in groundwater-dominated areas. For example, neither model variant is able to simulate flows adequately in the Mimram at Panshanger Park. This is probably because groundwater abstraction in the headwaters of the Mimram reduces observed flows below what would be expected naturally, leading to an apparent overestimate in the model simulations. For another low relief catchment in South East England affected by abstractions, the Thames to Kingston, naturalised observed flows are available in addition to gauged flows. Here, a comparison between naturalised and Soil-G2G modelled flows indicates that the representation of natural processes by the Soil-G2G model in groundwater-affected areas is reasonably good (Bell *et al.,* 2008).

Overall, the Soil-G2G model, which is supported by a range of digital datasets and has just one set of calibrated model parameters for the whole of the UK, simulates river flows reasonably well for a wide range of catchments. It performs very well for many catchments having a natural flow regime and for which the flow record is believed to be accurate. The Slope-G2G performs well for catchments where runoff-generation is controlled by topography and where terrain slope serves as a good surrogate for soil depth (absorption capacity). However, it is less effective in lowland areas where soil/geology controls can dominate the hydrological response. Model simulations (for both formulations) are less accurate in catchments where the flow regime is influenced by artificial abstractions and discharges, and where the sub-surface hydrology is unusually complex (and not well understood). A rainfall-runoff model calibrated to individual catchments can sometimes be adjusted to take such artificial influences into account, but this is not an option for an area-wide model constrained to use one set of model parameters for all locations. Future model development might include a scheme to incorporate losses due to groundwater abstraction, such as the groundwater model component developed for the PDM by Moore and Bell (2002).

Impact of hydrological model formulation on projected flow changes

Following the assessment of G2G model performance across the UK for a wide variety of catchments, the Slope-G2G and Soil-G2G are used next to investigate the impact of RCM-estimated climate change on flood magnitude across the UK. This allows an assessment to be made of the sensitivity of the estimated impacts to hydrological model structure. Estimates of spatial changes in peak flow, for different return periods, for river points on a 1km grid across the UK form the final output of this investigation into changing flood risk.

In order to be able to estimate flood frequency for each river point modelled by the G2G, annual maximum (AM) flows are stored for each point by UK water-year (1 October to 30 September). The AM are then ordered and their Gringorten (1963) plotting positions (estimates of the non-exceedence probability for each AM) determined. A generalised logistic distribution, recommended for UK catchments by Robson and Reed (1999), is then fitted to the AM at each point using L-moments. This method assumes stationarity over the data period and the fitted curve should not be used for extrapolation much beyond the data period length (in this case 30 years).

Fig. 7 maps the spatial changes in flood magnitude over the UK with river points colour-coded according to the percentage change in peak flow at 2, 10 and 20 year return periods. The maps in the first and second rows are derived using the Slope-G2G and Soil-G2G respectively. Red and orange colours indicate a decrease in peak flows under future climate conditions, blue and purple an increase, and yellow/green small decreases/increases. Overall, the maps of changes in peak flows from both G2G model variants are visually similar, particularly in high relief areas of North and West Britain. For South East England and the Midlands there is more spatial and inter-model variation in the estimated impact of climate change on river flows. These regions tend to have lower relief and spatially variable soil/geology and include areas where groundwater is a significant component of river flow. A large variation in percentage change in peak flows is apparent in individual river reaches (e.g. Thames, Severn), reflecting the differing response of subcatchments draining to them. Note that although the colour scale of Fig. 7 indicates projected decreases of over 60% and increases as high as 200% or more, there are very few of these areas in the Slope-G2G simulations and even fewer for the Soil-G2G. Most of the areas of high projected increases are located in Scotland or Northern England where the lack of an explicit snowmelt model may have led to some underestimation of Current flow peaks. This may have exaggerated the potential change in future flows as snowmelt events are expected to be less influential in a future warmer climate.

Maps of differences in percentage change between the two model variants (Soil-G2G – Slope-G2G), shown in the third row of Fig. 7, highlight that the largest areas of difference are in regions where slopes are lower and soils are particularly deep or shallow. Upland areas tend to be shaded in green which indicates very little difference between the models. Purple shading highlights areas where the Slope-G2G predicts a larger increase (or very occasionally a smaller decrease) than the Soil-G2G, and can coincide for example with regions of chalk or limestone geology. Orange areas are only apparent at higher return periods and tend to correspond to shallow soils in lowland regions for which the Soil-G2G predicts larger increases (or smaller decreases) than the Slope-G2G.

The G2G model assessment against river flow observations indicates that the Soil-G2G generally provides a more reliable flow simulation over low relief areas than the Slope-G2G, and also performs well over upland areas. The climate change impact results from this model might therefore be examined with greater confidence than those of the Slope-G2G. It is apparent from the maps in Fig. 7 obtained using the Soil-G2G model that the percentage change in future peak flows can vary between -60% and 100%. This is a very large range and it is worth considering some of the factors that are likely to be contributing to this degree of variability.

The maps of modelled changes in flood magnitude indicate decreases in some parts of South East England and the Midlands, particularly in areas overlying deeper soils and chalk bedrock. Clay soils can be relatively deep (although a shallow gleyed layer is often present), and while chalk soils are often quite thin, storage in areas underlain by chalk has been augmented in the Soil-G2G by increasing the soil depth. Conceptually this has the effect of introducing a deep unsaturated storage zone beneath the soil layer. A water balance analysis indicates that while the volumes of actual evaporation and total runoff are very similar for grid-cells in chalk and clay areas, the main difference between the two types of grid-cell is the time of release and partitioning of runoff between surface and sub-surface stores. In the G2G, areas with deeper stores respond more slowly to rainfall and evaporation than those with shallower ones such as clay because the release of water from the soil/unsaturated zone is determined by the relative saturation of the whole soil column. Areas with a deep soil/unsaturated layer (up to 3 m) seldom become completely saturated, resulting in slow release of water over several months. Under a future climate scenario of warmer drier summers and wetter winters, slowly-responding areas, such as chalk, are likely to “remember” the effects of a warm dry summer for many months as sub-surface storage and release is reduced. Chalk areas tend not to respond immediately to intense autumn/winter rainfall with high flows, but will instead replenish their stores. Projected increases in future evaporation may well extend the length of the autumn/winter period during which deep stores are replenished to field capacity. Catchments with shallower soils, such as upland, urban and clay areas, tend to respond immediately to high autumn/winter rainfall with high river flows, resulting in projected increases in future flow peaks. The ability of the Soil-G2G to reproduce these process-based mechanisms using historical observations gives greater weight to the model's projections of future change. The poorer performance of the Slope-G2G in simulating the timing and release of runoff in low-relief areas accounts for the difference in the two models' projections of peak flows in these areas. However, in higher-relief areas such as North and West Britain, both models can realistically simulate the hydrological response of catchments to rainfall, resulting in more-accurate simulation of observed flows and reasonable agreement on the likely effect of a future climate scenario on peak flows.

One of the most important factors influencing high river flows is rainfall. In the HadRM3H climate projections there are increases in rainfall across the UK in autumn/winter rainfall (which most influences peak flows in Britain (Bayliss and Jones, 1993)) of up to 30% across with significant regional differences. For England there are projected increases of up to 30% in winter rainfall, in Wales and Cornwall the projected increase is 10 to 20% and Northwest Scotland less than 10%. Fig. 7 indicates that the response to this projected climate change in Wales and Cornwall is an increase in peak flows, particularly at lower return periods, whilst in Western Scotland it is a decrease of up to 30%. This decrease is most likely to have arisen through a combination of a projected increase in future summer PE of up to 30%, and a decrease of up to 20% in future autumn rainfall with only a small increase in winter rainfall.

It is worth noting that saturation-excess runoff in soils is not the only mechanism leading to high river flows in the UK, although it is a key factor. Infiltration-capacity excess runoff occurs when intense rainfall exceeds the infiltration-capacity of the soil and can result in peak flows any time of the year, but particularly in summer months during localised convective storms. Infiltration-excess runoff is not included in the G2G formulations presented here, but further work might consider the effect of extremely intense rainfall on different types of soil and terrain. Extreme rainfall events caused by localised convection are not simulated by the 25 km resolution RCM and thus their effect on projected peak flows across the UK is uncertain.

It is important to note that some of the spatial variation in hydrological response could arise from "noise" in the RCM estimates of precipitation and PE used as input to the G2G hydrological model. When Bell *et al.* (2007b) used the same RCM to estimate the impact of climate change on flows in 25 catchments across the UK they noted that the rainfall simulated by the RCM over the first half of the Current period was affected by an unusually heavy rainfall event over southern England. The effect of one extreme rainfall event in the Current precipitation series was to raise the estimated peak flows for some catchments for high return periods. As the Future flow series did not contain a comparable flow peak, this significantly affected comparison of the flood frequency curves derived from the Current and Future flow simulations; removing the highest peak from the flood frequency analysis even resulted in changes of the opposite sign in some catchments. In order to investigate the robustness of the modelled changes in flood frequency here, particularly given the extreme rainfall event in the Current period for some areas, the resampling method followed by Bell *et al.* (2007b) was applied, on a point-by-point basis. That is, for each river point the AM series were resampled for both Current and Future periods with new flood frequency curves fitted to each resample. Specifically, the resampling at each location was undertaken 100,000 times with replacement, so that any one resampled series could contain some repeated AM and some absent. Percentage changes were then calculated between the new pairs of Current and Future curves at several return periods, and counts made of the number of pairs with changes of the same sign as the original.

The results are summarised in the set of maps in Fig. 8, which highlight areas for which most of the resamples keep the same direction of change in the future (increase or decrease in peak flows). More specifically, dark blue areas indicate areas for which more than 90% of the resampled AM series continue to show an increase in peak flows; dark red areas indicate areas where more than 90% show a decrease, and green and orange are the same as for blue and red respectively, but with only between 70% and 90% of the resamples in agreement. The maps indicate that, for both model formulations, changes at higher return periods are, unsurprisingly, generally less robust than those at lower return periods. However, this is particularly true for the Slope-G2G and over regions of south and east England, which were especially affected by the extreme rainfall event in the Current Period. For both G2G model variants, areas of change that are most robust are the wetter parts of the UK such as the north and west, perhaps because the AM are less variable in the wettest pasts of the country. Overall, the Soil-G2G is slightly more robust than the Slope-G2G, but the main differences between them lie in lowland areas such a South East England, for which the Soil-G2G is more realistic. In particular, at the 2-year return period the Slope-G2G indicates robust increases in many parts of South East England, but using the Soil-G2G some of these areas (such as those over chalk) instead show robust decreases. This highlights an important point that a "robust" model is not necessarily "correct", as robustness here tests only the homogeneity of the modelled flows, not the skill of the model to reproduce physical processes.

The robustness analysis has been repeated following removal of the highest peak from each AM series. The results shown in Fig. 9 indicate that, following removal of the highest peak, the sign of the percentage change in flood magnitude is robust for a larger area of the UK than shown in Fig. 8, with a particular difference for higher return periods and over South East England – the area affected by the extreme event in the Current period. These results highlight the importance of not giving too much weight to results obtained from just one Current and Future RCM scenario.

In terms of the modelled percentage changes in flood peaks between the Current and Future period, removal of the highest flow peak from the AM series and a subsequent recalculation of the flood frequency curves has a lesser effect on the Soil-G2G than the Slope-G2G, where it led to lower estimates of future decreases in flood magnitude in South East England. Performance of the Slope-G2G in low relief areas (such as the South East) is generally poorer than in upland areas and there is less confidence in projected change in this region.

Summary and discussion

A Grid-to-Grid (G2G) model has been calibrated to, and evaluated against, historical river flow data for catchments across Britain in order to obtain optimal model performance at a spatial resolution of 1km and a temporal resolution of one day (or less). Two formulations of the G2G are assessed using observations of rainfall, potential evaporation and daily mean river flow. Both model formulations are constrained to employ just one set of calibrated parameters for the whole of the UK and rely on digital datasets to provide spatially variable information on hydrological response. The Slope-G2G formulation performs well for catchments where runoff-generation is controlled by slope/topography, but is less effective where soil/geology is the dominant influence. The Soil-G2G model benefits from additional hydrological information contained in soil datasets and consequently simulates river flows reasonably well for a wide range of catchments, and very well for many catchments having a natural flow regime and for which the flow record is believed to be accurate.

Use of the grid-based methodology in conjunction with high resolution climate model output has made it possible here, for the first time, to estimate the spatial effects of climate change on peak river flows across the UK. The observations of rainfall and potential evaporation used to calibrate and assess both hydrological models were replaced by RCM estimates on a 25 km grid and at hourly intervals for a Current (1960 to 1990) and a Future (2070 to 2100) time-slice. Flood frequency curves were derived from the flow simulations obtained using the Current and Future precipitation estimates, and maps of estimated changes in flood magnitude for river points on a 1 km grid across the UK presented. These maps suggest a high degree of spatial variability in the sensitivity of UK rivers to future changes in climate, with the modelled percentage changes in future peak flows varying between -60% and 100% (sometimes outside of this range for the Slope-G2G). Climate change is only one factor responsible for these patterns of differences, with both landscape and internal climate variability being important factors. The very large range needs careful interpretation before clear messages about impacts of climate change on peak river flows can be drawn. It is important to recognise that in undertaking a hydrological impact analysis such as the one presented here, we assume that a model tested for current weather conditions will also apply under conditions associated with projected climate change. This reservation applies to almost any model used for climate change impact assessments, and we feel is most likely to be overcome with a process-based model, such as the Soil-G2G, tested over as wide a range of conditions as possible. This approach is also likely to lead to fewer problems related to over-calibration to current conditions and extrapolation than a catchment model which might only have been assessed on a small number of catchments.

The use of two different G2G model formulations allows us to assess the sensitivity of a climate impact flood risk assessment to hydrological model structure. Similarities between the results from both models are apparent, particularly in high relief areas such as the North and West of Britain. In South East England and the Midlands there is more spatial and inter-model variation in the estimated impact of climate change on river flows. These regions tend to have lower relief and spatially variable soil/geology and include areas where groundwater is a significant component of river flow. Analysis of the results in different regions highlights how the impact of climate change on river flows is likely to arise from a subtle combination of both local factors such as soil and relief, and a larger-scale fine balance between future seasonal change in rainfall and evaporation. Potential evaporation has been calculated here using a procedure as consistent as possible with a Penman-Monteith estimate. However, other methods of estimating PE are available and use of these could lead to different climate change impacts. Kay and Davies (2008), for example, obtain results that suggest a simple temperature-based estimator of PE may have benefit when calculated from climate model predicted variables. This may reflect the higher relative skill of climate models to predict temperature than other variables involved in the calculation of Penman-Monteith PE. Johnson and Sharma (2009) present climate model prediction results that ranks surface air temperature as second highest only to pressure in skill. Rain rate is ranked least skilful of the eight climate variables assessed. This uncertainty presents a well known challenge for climate modellers that is being addressed here through the use of a high-resolution RCM, and through ensembles in other work. Maps of percentage change in HadRM3H Penman-Monteith PE (not shown) indicate a future increase across the whole of the UK, with the greatest increase occurring in the South. However, any future increase in carbon dioxide might instead lead to a decrease in plant transpiration and a greater propensity for high river flows (Gedney *et al.*, 2006), a factor which has not been included in the analysis presented here.

An analysis of the robustness of the sign of the changes in flood magnitude indicated that, for both G2G model formulations, areas of change that are most robust are the wetter parts of the UK such as the north and west, perhaps because the annual maxima are less variable here. Also, larger areas of robust peak flow changes are seen using the Soil-G2G with the main differences between the two models occurring in lowland areas such as South East England. Here the simulation-performance of the Soil-G2G is more realistic and thus these results are likely to be more reliable.

Results in the South East were also skewed by the presence of an extreme rainfall event in the Current period, highlighting the importance of not giving too much weight to results obtained from a single 30-year sample of a Current and Future climate period. Ideally using an ensemble approach to fully sample the climatologies of the two periods (Kendon et al, 2008) would be applied. Possible alternatives when modelling individual catchments could be to apply a weather generator (e.g. Kilsby *et al.,* 2007) or to resample the available rainfall inputs a large number of times (e.g. Kay *et al.,* 2009), but the need here for spatially-consistent rainfall across the UK currently precludes the use of the former, and the fact that the G2G currently takes 3 weeks to run for a 30-year time-slice on a 1km grid across the UK precludes the latter.

The use of two different model variants employing the same climate model estimates of precipitation and PE as input has highlighted the importance of using the most accurate, physically representative model as possible for climate impact assessments. Different hydrological models can respond in unexpected ways to subtle changes in the climate model estimates used as input. The results presented here indicate that the effect of projected climate change on UK catchments is sensitive not only to changes in the precipitation and PE data used as input, but to the model representations used to capture "traditional" hydrological responses. Future research will therefore aim to improve process-representation in the G2G model in order to increase confidence in simulated projected changes in peak river flows. Snowmelt, for example, is an important influence on river flows which is not currently included in the G2G, and the lack of a snowmelt representation is likely to have led to an exaggeration in the estimated impact of climate change on river flows in upland areas. Similarly, processes such as flood-plain storage and attenuation which influence the occurrence of flood inundation are not currently included. Flood-plain storage has the effect of reducing the intensity of high river flows, and large percentage changes in estimated future peak flows would in practice be reduced if current levels of available storage are maintained. The maps of changing flood risk presented here reveal the spatial complexity of the response of UK catchments to one particular projected climate change. However, to support flood management and policy decisions concerning key catchments, a more comprehensive analysis is needed taking into account relevant hydrological processes and embracing consideration of catchment conditions, multiple climate scenarios and climate model structure at different scales.

Acknowledgements

This research was funded via the UK Met Office Hadley Centre by the Joint Department of Energy and Climate Change and Ministry of Defence Integrated Climate Programme: (DECC) GA01101 (MoD) CBC/2B/0417_Annex C5. Additional support was provided by the CEH Science Programme and the NERC Flood Risk from Extreme Events (FREE) Programme. The authors would like to thank Terry Marsh at CEH Wallingford for helpful advice and discussions concerning UK catchments, gauging stations and observational evidence for flood trends.

References

Arnell, N.W., 2003. Relative effects of multi-decadal climatic variability and changes in the mean and variability of climate due to global warming: future streamflows in Britain. Journal of Hydrology 270, 195–213.

Bayliss, A.C., Jones, R.C., 1993. Peaks-over-threshold flood database – summary statistics and seasonality. IH Report No. 121, Institute of Hydrology, Wallingford, UK.

Bell, V.A., Moore, R.J., Cole, S.J., Davies, H.N., 2008. Area-wide river flow modelling for the Thames Estuary 2100 project: Model formulation and assessment. Progress Report to the Met Office (Hadley Centre). Centre for Ecology and Hydrology, Wallingford, UK, 69pp.

Bell V.A., Kay A.L., Jones R.G., Moore R.J., 2007a. Development of a high resolution grid-based river flow model for use with regional climate model output. Hydrology and Earth System Sciences 11(1), 532-549.

Bell, V.A., Kay, A.L., Jones, R.G., Moore, R.J., 2007b. Use of a grid-based hydrological model and regional climate model outputs to assess changing flood risk. International Journal of Climatology 27, 1657-1671.

Bell, V.A., Moore, R.J., 2004. A flow routing and flood inundation facility for Nimrod/CMetS. Report to the Met Office. Centre for Ecology and Hydrology, Wallingford, UK, 56pp.

Bell V.A., Moore R.J., 1998a. A grid-based distributed flood forecasting model for use with weather radar data. Part 1: Formulation. Hydrology and Earth System Sciences 2(2-3), 265-281.

Bell V.A., Moore R.J., 1998b. A grid-based distributed flood forecasting model for use with weather radar data. Part 2: Case Studies. Hydrology and Earth System Sciences 2(2-3), 283-278.

Benning, R.G., 1995. Towards a new lumped parameterisation at catchment scale. Report 54, Department of Water Resources, Agricultural University, Wageningen, The Netherlands, 60pp plus Appendices and Tables.

Black, A.R., 1996. Major flooding and increased flood frequency in Scotland since 1988. Phys. Chem. Earth 20, 463-468.

Boorman, D.B., Hollis, J.M., Lilly, A., 1995. Hydrology of soil types: a hydrologically based classification of the soils of the United Kingdom. IH Report No. 126, Institute of Hydrology, Wallingford, UK, 137pp.

Brooks, R.H., Corey, A.T., 1964. Hydraulic properties of porous media. Hydrology Paper 3, Colorado State University, Fort Collins, USA.

Buonomo, E., Jones, R.G., Huntingford, C., Hannaford, J., 2007. On the robustness of changes in extreme precipitation over Europe from two high resolution climate change simulations. Quarterly Journal of the Royal Meteorological Society 133(622), 65-81.

Burrough, P., 1986. Principles of Geographic Information Systems for Land Resources Assessment. Monograph on Soil and Resources Survey No. 12. Clarendon Press, Oxford, UK, 194 pp.

Cameron, D., 2006. An application of the UKCIP02 scenarios to flood estimation by continuous simulation for a gauged catchment in the northeast of Scotland, UK (with uncertainty). Journal of Hydrology 328, 212-226.

Ciarapica, L., Todini, E., 2002. TOPKAPI: a model for the representation of the rainfall - runoff process at different scales. Hydrological Processes 16, 207 – 229.

Clapp, R.B., Hornberger, G.M., 1978. Empirical equations for some soil hydraulic properties. Water Resources Research 14(4), 601-604.

Davies, H.N., Bell, V.A., 2009. Assessment of methods for extracting low-resolution river networks from high-resolution digital data. Hydrological Sciences Journal 54(1), 17-28.

Defra, 2006. Flood and Coastal Defence Appraisal Guidance: FCDPAG3 Economic appraisal. Supplementary note to operating authorities: Climate change impacts. October 2006. (http://www.defra.gov.uk/environ/fcd/pubs/pagn/climatechangeupdate.pdf)

Dooge, J.C.I., 1973. Linear theory of hydrologic systems. Tech. Bull. 1468, Agric. Res. Service, US Dept. Agric., Washington, USA, 327pp.

Dunne, T., Leopold, L.B., 1978. Water in Environmental Planning. W.H. Freeman and Company, New York, 817 pp.

Fekete, B., Vorosmarty, C., Lammers, R., 2001. Scaling gridded river networks for macroscale hydrology: Development, analysis and control of error. Water Resour. Res. 37(7), 1955-1967.

Fowler, H., Ekström M., Kilsby, C., Jones, P.D., 2005. New estimates of future changes in extreme rainfall across the UK using regional climate model integrations. 1: Assessment of control climate. Journal of Hydrology 300(1-4), 212-233.

Fowler, H.J., Kilsby, C.G., 2007. Using regional climate model data to simulate historical and future river flows in northwest England. Climatic Change 80(3-4), 337-367.

Fuller, R.M., Smith, G.M., Sanderson, J.M., Hill, R.A., Thomson, A.G., 2002. The UK Land Cover Map 2000: Construction of a parcel-based vector map from satellite images. Cartographic Journal 39(1), 15-25.

Gedney, N., Cox, P.M., Betts, R.A., Boucher, O., Huntingford, C.. Stott, P.A., 2006. Detection of a direct carbon dioxide effect in continental river runoff records. Nature 439, 835-838.

Gringorten, L.J., 1963. A plotting rule for extreme probability paper. Journal of Geophysical Research 68(3), 813–814.

Hallett, S.H., Thanigasalam, P., Hollis, J.M., 1995. SEISMIC: a desktop information system for assessing the fate and behaviour of pesticides in the environment. Computers and Electronics in Agriculture 13, 227-242.

Hannaford J. and Marsh T., 2008. High-flow and flood trends in a network of undisturbed catchments in the UK. International Journal of Climatology 28, 1325-1338.

Hough MN, Jones RJA. 1997. The United Kingdom Meteorological Office rainfall and evaporation calculation system: MORECS version 2.0 – an overview. Hydrology and Earth System Sciences 1, 227-239.

Hulme, M., Jenkins, G., Lu, X., Turnpenny, J., Mitchell, T., Jones, R., Lowe, J., Murphy, J., Hassell, D., Boorman, P., Macdonald, R., Hill, S., 2002. Climate-Change Scenarios for the United Kingdom: The UKCIP02 Scientific Report. Tyndall Centre for Climate Change Research, School of Environmental Sciences, University of East Anglia, Norwich, UK, 120pp.

Institute of Hydrology. 1980. Low flow studies report. Institute of Hydrology, Wallingford, UK.

IPCC, 2000. Special report on emissions scenarios (SRES): a special report of working group III of the intergovernmental panel on climate change. Cambridge University Press, Cambridge, UK, 570pp.

Johnson, F., Sharma, A., 2009. Measurement of GCM skill in predicting variables relevant for hydroclimatological assessments. Journal of Climate, in press, doi: 10.1175/2009JCLI2681.1.

Kay, A.L., Jones, R.G., Reynard, N.S. 2006. RCM rainfall for UK flood frequency estimation. II. Climate change results. .Journal of Hydrology 318, 163-172.

Kay, A.L., Davies, H.N., 2008. Calculating potential evaporation from climate model data: a source of uncertainty for hydrological climate change impacts. Journal of Hydrology 358, 221– 239, doi: 10.1016/j.jhydrol.2008.06.005.

Kay, A.L., Davies, H.N., Bell, V.A., Jones, R.G., 2009. Comparison of uncertainty sources for climate change impacts: flood frequency in England. Climatic Change, 92(1-2), 41-63, doi: 10.1007/s10584-008-9471-4

Kilsby, C.G., Jones, P.D., Burton, A., Ford, A.C., Fowler, H.J., Harpham, C., James, P., Smith, A., Wilby, R.L., 2007. A daily weather generator for use in climate change studies. Envir. Model. Softw. 22(12), 1705-1719.

Liu, Z., Martina, M.L.V., Todini, E., 2005. Flood forecasting using a fully distributed model: application of the TOPKAPI model to the Upper Xixian Catchment. Hydrol. Earth System Sci. 9(4), 347–364.

Monteith, J.L., 1965. Evaporation and environment. Symp. Soc. Exp. Biol. 19, 205-234.

Moore, R.J., 1985. The probability-distributed principle and runoff production at point and basin scales. Hydrol. Sci. J. 30(2), 273-297.

Moore. R.J., 2007. The PDM rainfall-runoff model. Hydrology and Earth System Sciences 11(1), 483-499.

Moore, R.J., Bell, V.A., 2001. Comparison of rainfall-runoff models for flood forecasting. Part 1: Literature review of models. Environment Agency Research and Development Technical Report W241, Research Contractor: CEH Wallingford, Environment Agency, 94pp.

Moore, R.J., Bell, V.A., 2002. Incorporation of groundwater losses and well level data in rainfall-runoff models illustrated using the PDM. Hydrology and Earth System Sciences 6(1), 25-38.

Moore, R.J., Bell, V.A., Cole, S.J., Jones, D.A., 2006a. Spatio-temporal rainfall datasets and their use in evaluating the extreme event performance of hydrological models. R&D Project Report FD2208/PR, Joint Defra/Environment Agency Flood and Costal Erosion Risk Management, Research Contractor: CEH Wallingford, Defra, 259pp. (Web link: http://nora.nerc.ac.uk/2187/)

Moore R.J., Cole S.J., Bell V.A., Jones D.A., 2006b. Issues in flood forecasting: ungauged basins, extreme floods and uncertainty. In: I. Tchiguirinskaia, K. N. N. Thein, P. Hubert (eds.), Frontiers in Flood Research, 8th Kovacs Colloquium, UNESCO, Paris, June/July 2006, IAHS Publ. 305, 103-122.

Moore, R.J., Bell, V.A., Cole, S.J., Jones, D.A., 2007. Rainfall-runoff and other modelling for ungauged/low-benefit locations. R&D Project W5-113, Report to the Environment Agency and Defra, CEH Wallingford, 249pp. (Web link: http://nora.nerc.ac.uk/1134/)

Morris, D.G., Flavin, R.W., 1990. A digital terrain model for hydrology. Proceedings 4th International Symposium on Spatial Data Handling, 23-27 July, Zürich, Vol. 1, 250-262.

Nash, J.E., Sutcliffe, J.V., 1970. River flow forecasting through conceptual models, Part I: a discussion of principles. Journal of Hydrology 10(3), 282–290.

Nawaz, N.R., Adeloye, A.J., 2006. Monte Carlo assessment of sampling uncertainty of climate change impacts on water resources yield in Yorkshire, England. Climatic Change 78, 257-292.

New, M., Lopez, A., Dessai, S., Wilby, R., 2007. Challenges in using probabilistic climate change information for impact assessments: an example from the water sector. Philosophical Transactions of the Royal Society Series A 365, 2117-2131.

Nixon, M., 1959. A study of the bank-full discharges of rivers in England and Wales. Proceedings of the Institution of Civil Engineers 12, 157-194.

Or, D., Wraith, J.M., 2002. Soil water content and water potential relationships. In: Warrick, A.W. (ed.), Soil physics companion, CRC Press, Boca Rouge, USA, 49-84.

Osborn, T.J., Hulme, M., 2002. Evidence for trends in heavy rainfall events over the United Kingdom. Philosophical Transactions of the Royal Society Series A, 360, 1313-1325. doi:10.1098/rsta.2002.1002.

Paz, A.R., Collischonn, W., Lopes da Silveira, A.L., 2006. Improvements in large-scale drainage networks derived from digital elevation models. Water Resources Research **42**(8), W08502, doi:10.1029/2005WR004544.

Reynard, N.S., Crooks, S.M., Kay, A.L., 2004. Impact of climate change on flood flows in river catchments. Report to the UK Department for Environment, Food and Rural Affairs and the Environment Agency, Project W5B-032 final report, Centre for Ecology and Hydrology, Wallingford, UK, 97pp.

Robson, A.J., Reed, D.W., 1999. Statistical procedures for flood frequency estimation. Vol. 3, Flood Estimation Handbook. Institute of Hydrology, Wallingford, UK, 338pp.

Robson, A.J., 2002. Evidence for trends in UK flooding. Philosophical Transactions of the Royal Society Series A 360, 1327-1343.

Smith, J.M., 1977. Mathematical modelling and digital simulation for engineers and scientists. J. Wiley, New York, USA, 332 pp.

Thompson, N., Barrie, I.A., Ayles, M., 1981. The Meteorological Office Rainfall and Evaporation Calculation System: MORECS (July 1981). Hydrological Memorandum No. 45, Met Office, Bracknell, UK.

Todini, E., 1995. New trends in modelling soil processes from hillslope to GCM scales. In: H.R. Oliver and S. A. Oliver (eds.), The role of water and the hydrological cycle in global change. NATO ASI Series I 31, 317-347, Springer-Verlag, Berlin, Germany.

Todini, E., 1996. The ARNO rainfall-runoff model. Journal of Hydrology 175, 339-382.

Wilby, R.L., Harris, I., 2006. A framework for assessing uncertainties in climate change impacts: Low-flow scenarios for the River Thames, UK. Water Resources Research 42, W02419, doi: 10.1029/2005WR004065.

Wilby, R.L., Whitehead, P.G., Wade, A.J., Butterfield, D., Davis, R.J., Watts, G., 2006. Integrated modelling of climate change impacts on water resources and quality in a lowland catchment: River Kennet, UK. Journal of Hydrology 330, 204-220.

Wood, E.F., Lettenmaier, D.P. Zartarian, V.G., 1992. A land surface hydrology parameterization with subgrid variability for general circulation models. Journal of Geophysical Research 97(3), 2717–2728.

Zhao, R.J., Zuang, Y.L., Fang, L.R., Liu X.R., Zhang Q.S. 1980. The Xinanjiang model. In: Hydrological forecasting (Proceedings. Oxford Symposium, April 1980), IAHS Publication 129, 351-356.

FIGURES AND TABLES

Figure 1. Conceptual diagram showing runoff production and lateral drainage in a 1-D soil column.

Figure 2. Relationship between PDM distribution parameter, b, and the catchment maximum store capacity, $S'_{\max}$, for a range of UK catchments.

Figure 3. Key features of the coupled runoff-production and routing scheme.

Figure 4. Location of the UK catchments used for G2G model assessment (labelled by station ID – see Table 1).

Figure 5. Comparison of R^2 model performance, ordered in terms of increasing *bfi*, using two G2G formulations to model daily river flow for 42 catchments across the UK: 1 January 1985 to 31 December 1993. Negative R^2 values are indicated with a nominal value of -0.05 for clarity.

Figure 6. Flow hydrographs comparing model performance from the Slope-G2G and Soil-G2G: 1 January 1985 to 31 December 1986.

Figure 7. Percentage change in flood magnitude, for three return periods, across the UK.

Figure 8. Robustness of the estimated changes in flood magnitude, for three return periods, for the Slope-G2G and the Soil-G2G model variants.

Figure 9. Robustness of the estimated changes in flood magnitude, for three return periods, for the Slope-G2G and the Soil-G2G, following removal of the highest peak from each AM series.

Table 1. UK catchments used for model assessment.

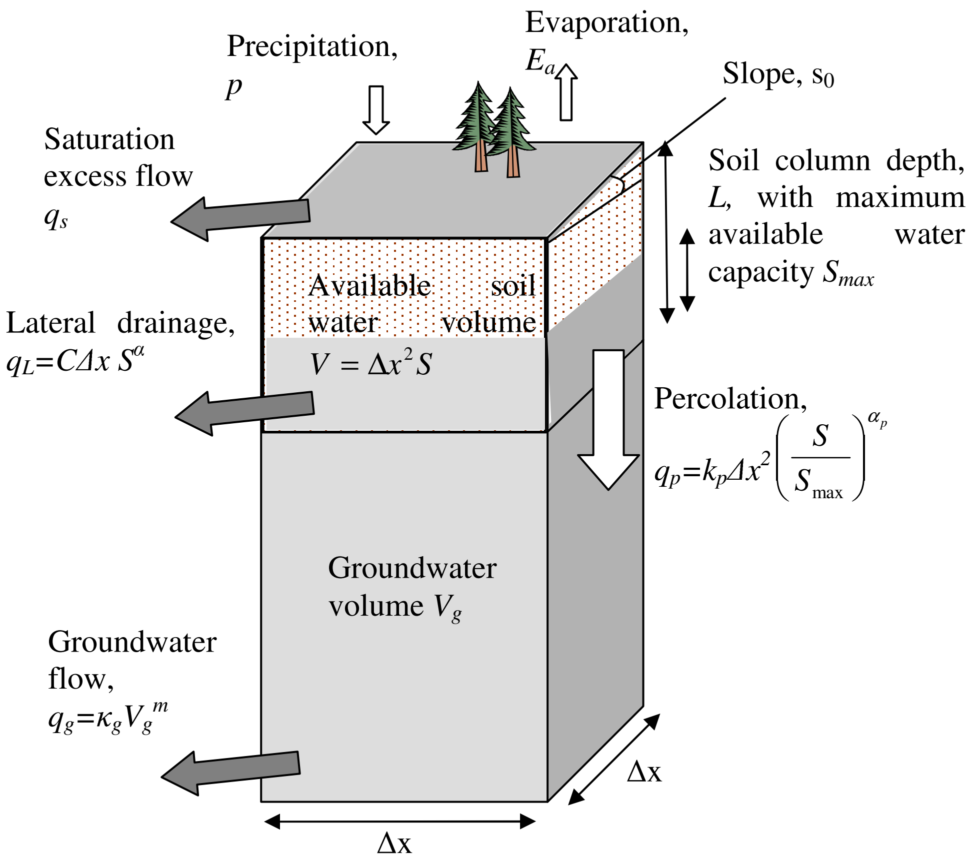
Precipitation,
p
Evaporation,
E_a
Slope, s_0
Saturation excess flow
q_s
Soil column depth, L, with maximum available water capacity S_{max}
Available soil water volume
$V = \Delta x^2 S$
Lateral drainage,
$q_L = C\Delta x\, S^{\alpha}$
Percolation,
$q_p = k_p \Delta x^2 \left(\frac{S}{S_{\max}}\right)^{\alpha_p}$
Groundwater volume V_g
Groundwater flow,
$q_g = \kappa_g V_g^{\,m}$
Δx
Δx

Figure 1

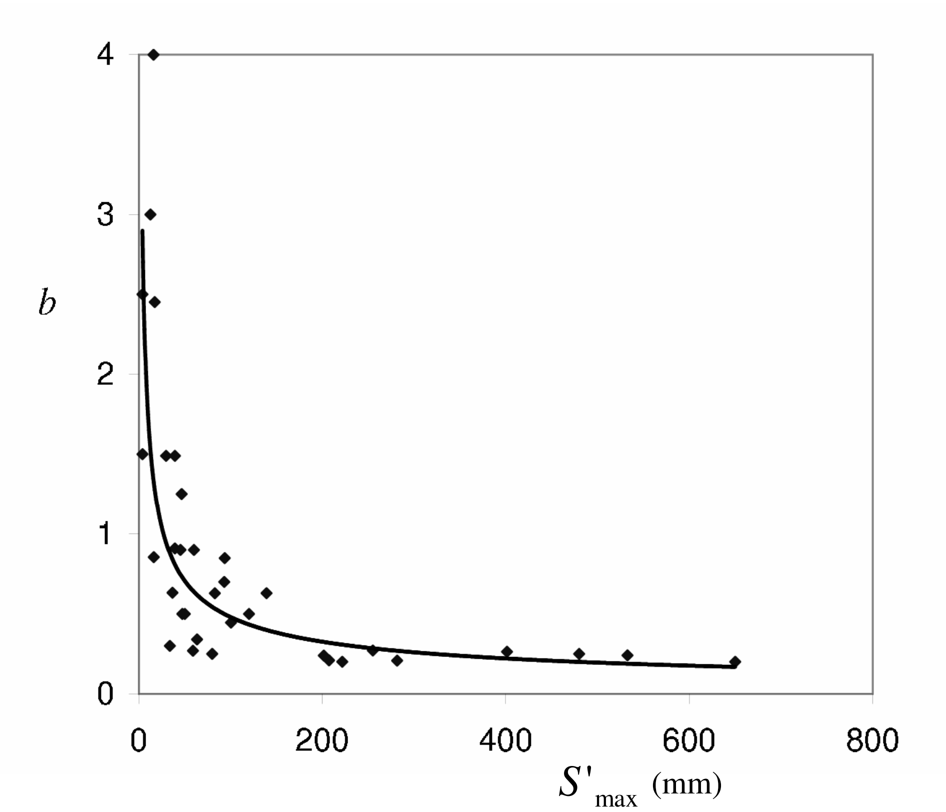

Figure 2

Figure3

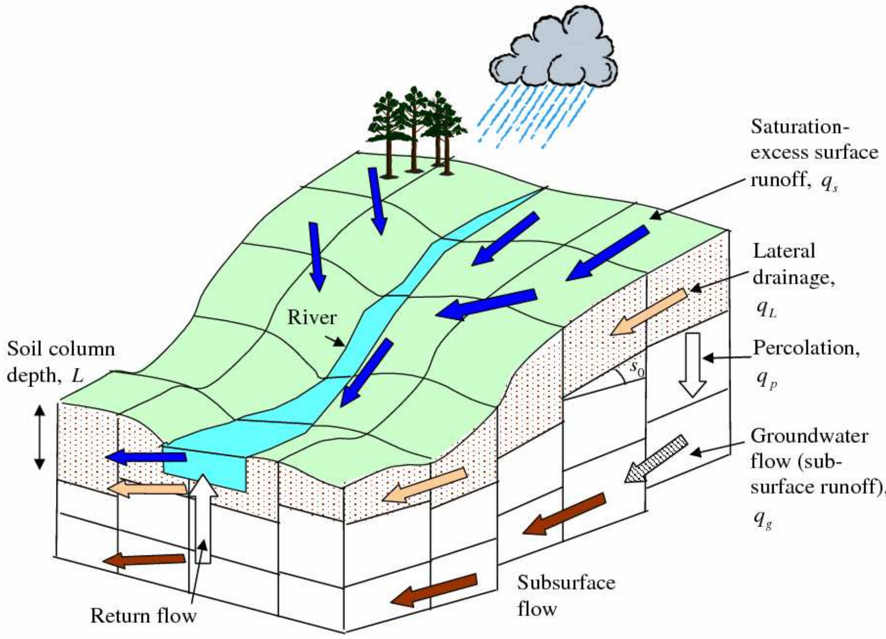

Saturation-excess surface runoff, q_s
Lateral drainage, q_L
Percolation, q_p
Groundwater flow (sub-surface runoff), q_g
s_0
River
Soil column depth, L
Return flow
Subsurface flow

Figure 4

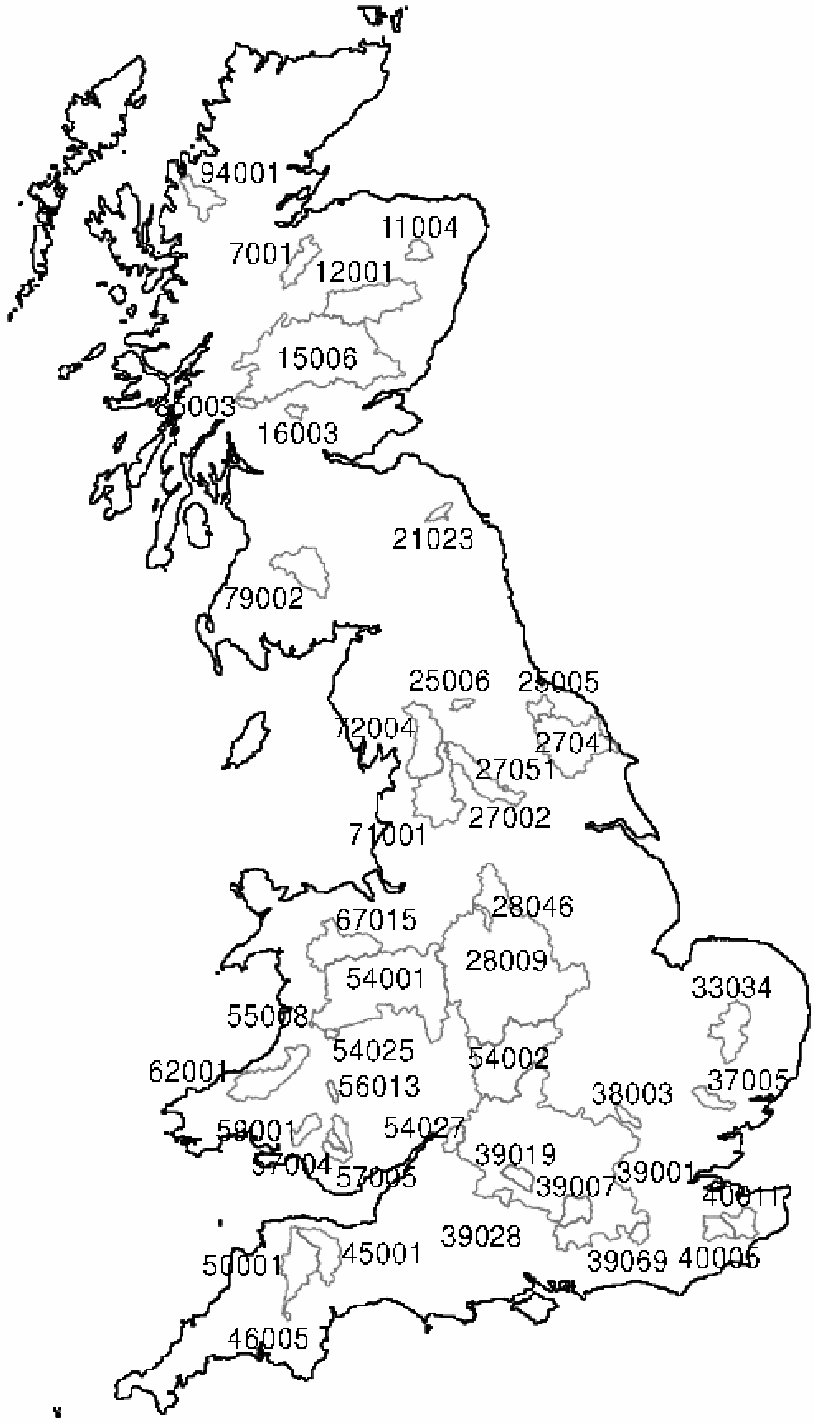
94001
11004
7001
12001
15006
16003
21023
79002
25006
25005
72004
27041
27051
27002
71001
28046
67015
28009
54001
33034
55008
54025
54002
62001
56013
38003
37005
59001
54027
39019
57004
57005
39007
39001
40011
39028
45001
50001
39069
40006
46005

Figure 5

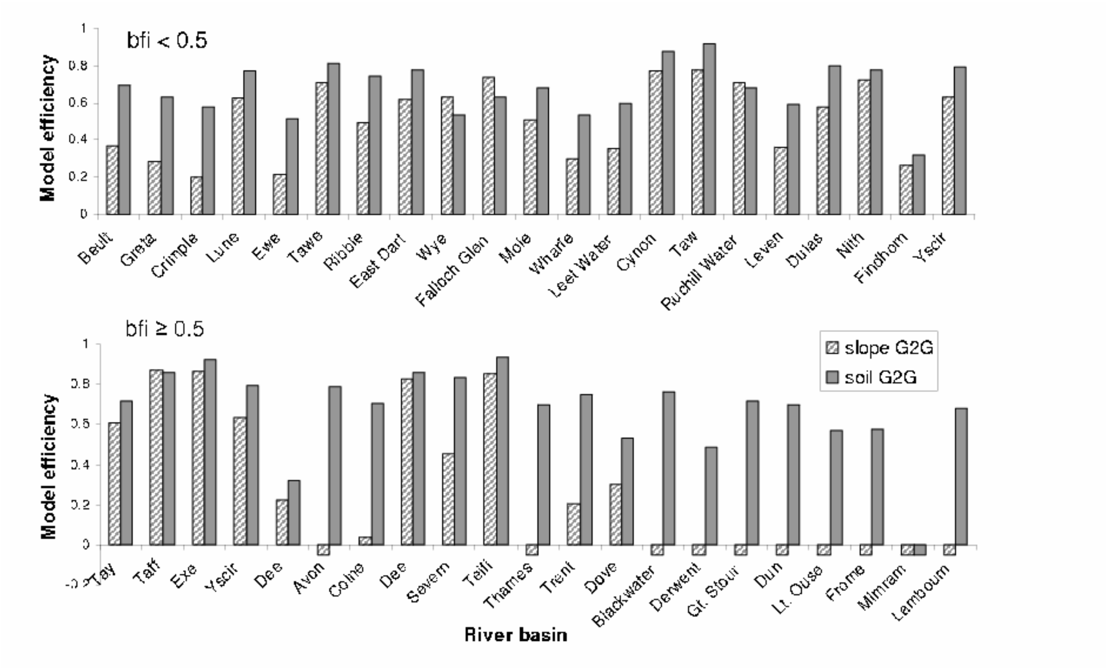
bfi < 0.5
Model efficiency
0
0.2
0.4
0.6
0.8
1
Beult
Greta
Crimple
Lune
Ewe
Tawe
Ribble
East Dart
Wye
Falloch Glen
Mole
Wharfe
Leet Water
Cynon
Taw
Ruchill Water
Leven
Dulas
Nith
Findhorn
Yscir
bfi ≥ 0.5
slope G2G
soil G2G
Tay
Taff
Exe
Yscir
Dee
Avon
Colne
Dee
Severn
Teifi
Thames
Trent
Dove
Blackwater
Derwent
Gt. Stour
Dun
Lt. Ouse
Frome
Mimram
Lambourn
River basin

Figure 6

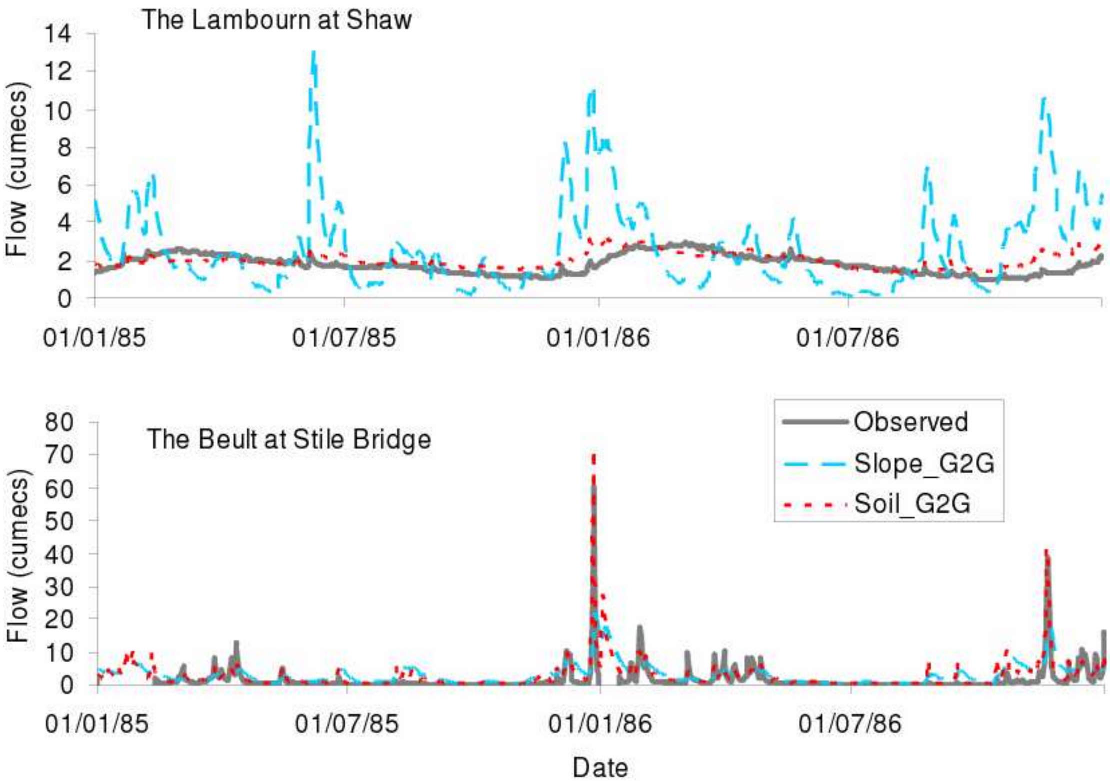
The Lambourn at Shaw
Flow (cumecs)
0
2
4
6
8
10
12
14
01/01/85
01/07/85
01/01/86
01/07/86
The Beult at Stile Bridge
Flow (cumecs)
0
10
20
30
40
50
60
70
80
Observed
Slope_G2G
Soil_G2G
01/01/85
01/07/85
01/01/86
01/07/86
Date

Figure 7

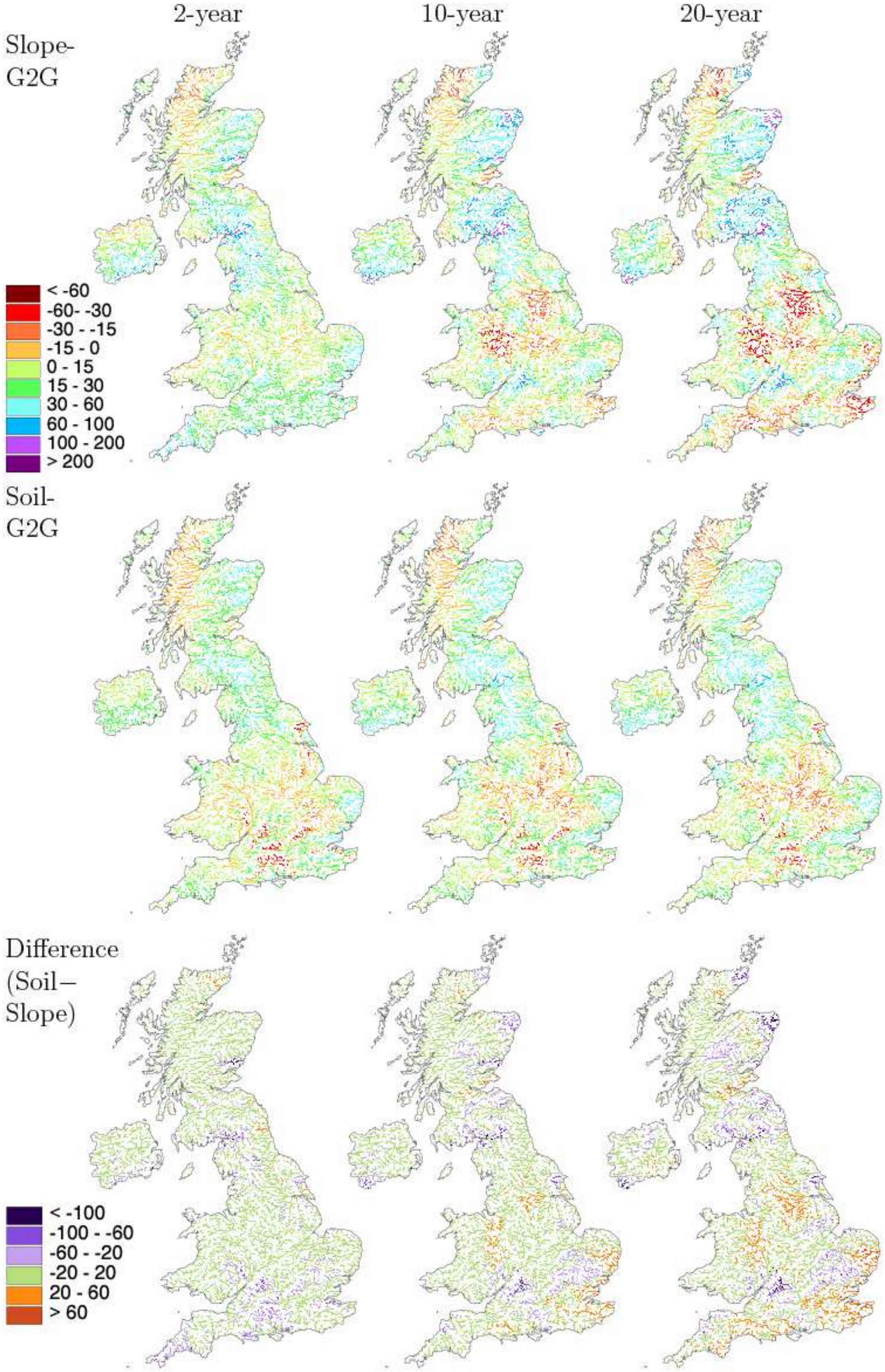

2-year
10-year
20-year
Slope-G2G
< -60
-60- -30
-30 - -15
-15 - 0
0 - 15
15 - 30
30 - 60
60 - 100
100 - 200
> 200
Soil-G2G
Difference (Soil−Slope)
< -100
-100 - -60
-60 - -20
-20 - 20
20 - 60
> 60

Figure 8

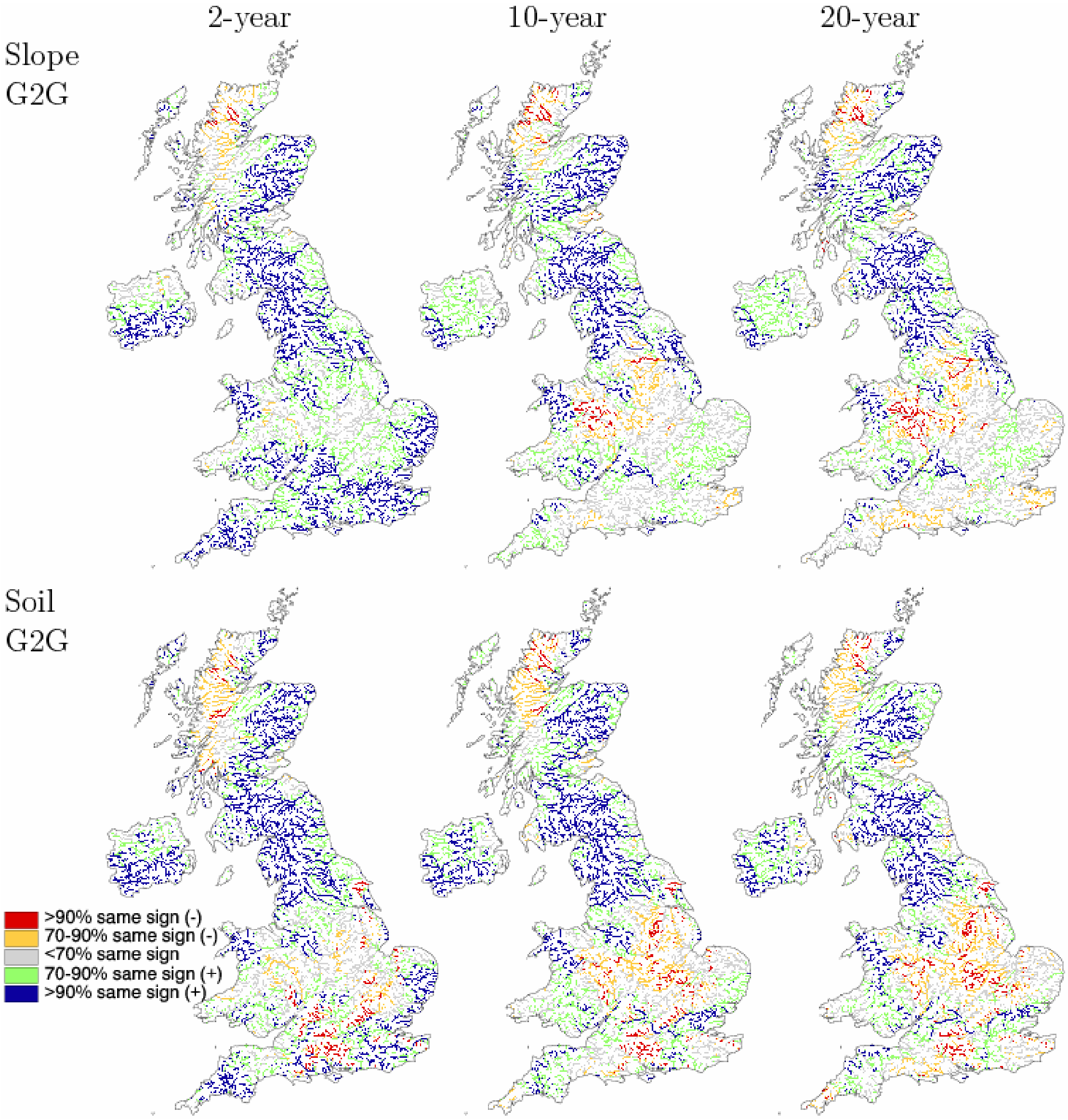
2-year
10-year
20-year
Slope
G2G
Soil
G2G
>90% same sign (-)
70-90% same sign (-)
<70% same sign
70-90% same sign (+)
>90% same sign (+)

Figure 9

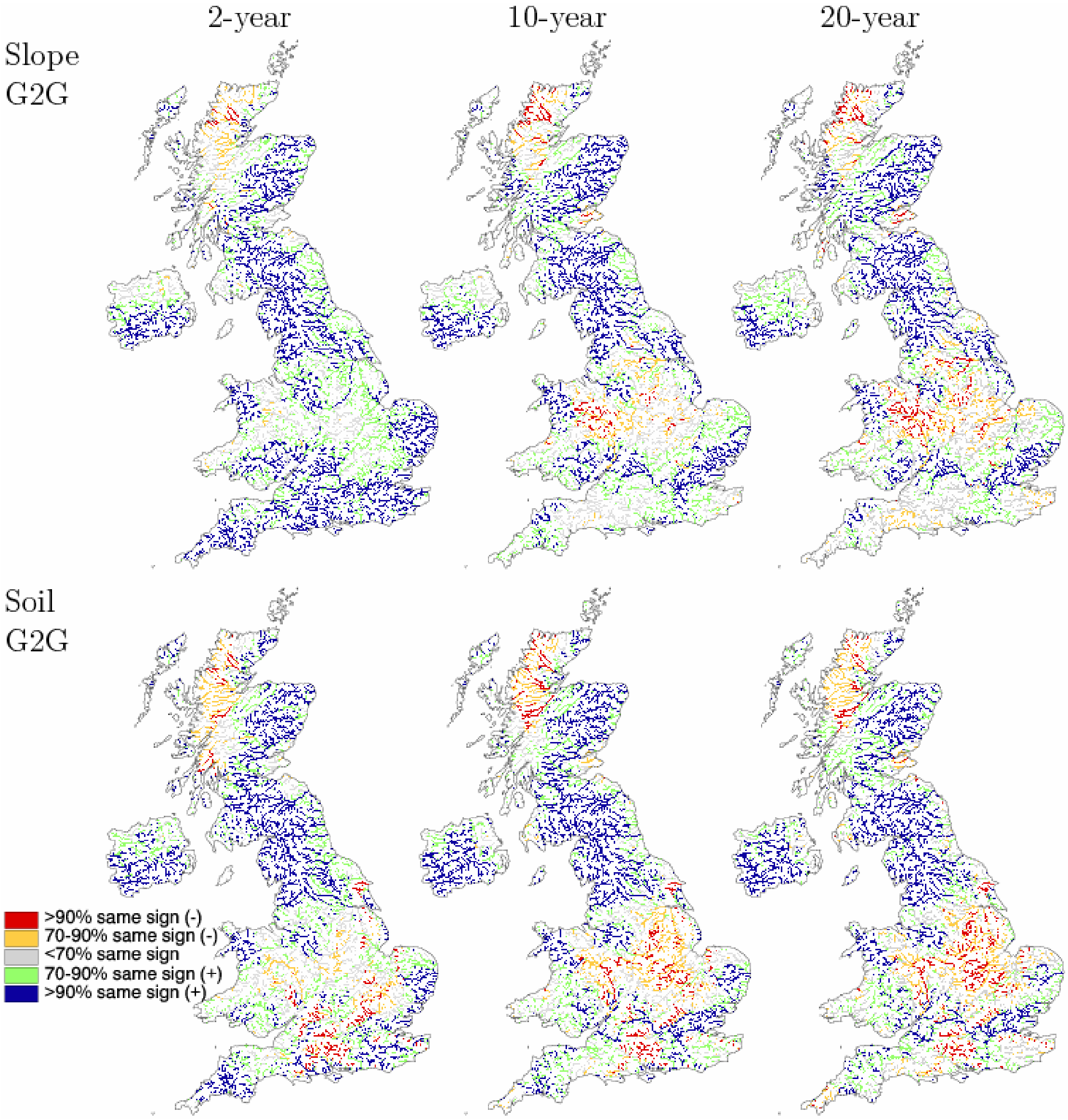
2-year
10-year
20-year
Slope
G2G
Soil
G2G
>90% same sign (-)
70-90% same sign (-)
<70% same sign
70-90% same sign (+)
>90% same sign (+)